Linear Wave Dynamics Explains Observations Attributed to Dark Solitons in a Polariton Quantum Fluid

P. Cilibrizzi,[1] H. Ohadi,[1] T. Ostatnicky,[2] A. Askitopoulos,[1] W. Langbein,[3] and P. Lagoudakis[1,*]
[1]School of Physics and Astronomy, University of Southampton, Southampton SO17 1BJ, United Kingdom
[2]Faculty of Mathematics and Physics, Charles University in Prague, Ke Karlovu 3, 121 15 Prague, Czech Republic
[3]School of Physics and Astronomy, Cardiff University, The Parade, CF24 3AA Cardiff, United Kingdom
(Received 11 June 2013; published 3 September 2014)

We investigate the propagation and scattering of polaritons in a planar GaAs microcavity in the linear regime under resonant excitation. The propagation of the coherent polariton wave across an extended defect creates phase and intensity patterns with identical qualitative features previously attributed to dark and half-dark solitons of polaritons. We demonstrate that these features are observed for negligible nonlinearity (i.e., polariton-polariton interaction) and are, therefore, not sufficient to identify dark and half-dark solitons. A linear model based on the Maxwell equations is shown to reproduce the experimental observations.

DOI: 10.1103/PhysRevLett.113.103901 PACS numbers: 42.65.Tg, 03.75.Lm, 42.25.Fx, 47.35.Fg

Solitons are solitary waves that preserve their shape while propagating through a dispersive medium [1,2] due to the compensation of the dispersion-induced broadening by the nonlinearity of the medium [3]. Over the years, spatial solitons have been observed by employing a variety of nonlinearities ranging from Kerr nonlinear media [4] to photorefractive [5] and quadratic [6] materials. Apart from their potential application in optical communications [7,8], solitons are important features of interacting Bose-Einstein condensates (BECs) and superfluids. The nonlinear properties of BECs can give rise to the formation of quantized interacting vortices and solitons, the latter resulting from the cancellation of the dispersion by interactions, for example, in atomic condensates. A special class of solitons is the so-called dark soliton, which feature a density node accompanied by a π phase jump. Since the first theoretical prediction in the context of BECs [9], dark solitons were studied and observed first in the field of nonlinear optics [10] and, then, in cold-atom BECs [11]. The experimental observation of BECs [12] and superfluidity [13,14] of exciton-polaritons, has sparked interest in the quantum-hydrodynamic properties of polariton fluids. In particular, the nucleation of solitary waves in the wake of an obstacle (i.e., defect) has been claimed recently [15–19]. Here, the source of nonlinearity, essential for the formation of such a solitary wave, has been identified in the repulsive polariton-polariton interactions. In these previous works, the observation of dark notches in the intensity profiles together with a π shift in the phase have been used as sufficient signatures for dark solitons in microcavities. In addition, half-dark solitons have been reported to carry a nonzero degree of circular polarization in the presence of the TE-TM splitting of the cavity mode [19].

In this Letter, we demonstrate that these features, used as dark-soliton fingerprints [15–19], can also be observed without the presence of nonlinearity, which is the fundamental ingredient differentiating solitons from linear wave propagation. Specifically, we investigate the propagation of polaritons with a small exciton fraction and at low polariton densities, excluding a relevant influence of nonlinearities. We show that polariton propagation in this linear regime across an extended defect can create deep notches in the intensity profile accompanied by a π phase shift. We model the observation using linear wave propagation, clarifying that these features are not indicative of a nonlinear interaction between polaritons, but are interference patterns created by scattering from the defect. Moreover, we show that the appearance or disappearance of these features for different in-plane kinetic energies is found also in the linear regime and, thus, does not provide evidence of an interacting quantum fluid. Therefore, the previous reports of the observation of dark solitons [15–18] and half-dark-solitons [19], which were based on these features, have to be reconsidered.

The investigated sample is a bulk λ GaAs microcavity surrounded by 27 (top) and 24 (bottom) distributed GaAs/AlAs Bragg reflector pairs. The sample is held in a cold-finger cryostat at a temperature of 15 K and is illuminated by a narrow linewidth single-mode continuous wave laser, tuned to the resonance of the cavity at about 1.485 eV. The measurements were performed in transmission configuration. The phase was measured using a shearing Mach-Zehnder interferometer (see [20], S1). Our experiments were performed in the linear regime, facilitated by the large negative detuning of -29 meV of the cavity photon mode from the exciton resonance at 1.514 eV, resulting in a small exciton fraction of the polariton of about 1%. To verify the linear regime, we studied the excitation density dependence of our results with both a Gaussian and half-Gaussian excitation beam (see [20], S2). We find that they are independent of both the shape of the beam and the excitation density over a range of 4 orders of magnitude

and they persist at polariton density as low as 2.3×10^2 cm^{-2}, 7 orders of magnitude lower than the lasing threshold observed in standard microcavities [21].

The real space intensity and interference of a polariton wave propagating across a defect are shown in Fig. 1. The experimental results show the presence of two dark notches in the intensity pattern along with a π phase shift visible in Fig. 1(b) as paths of vortices merging in succession with alternating topological charge ± 1. Simulations of the measurements using the realistic experimental parameters are shown in Figs. 1(c) and 1(d).

Solitons are predicted to appear in polariton microcavities as the result of the nonlinearity due to the polariton-polariton interactions [22]. Since our experiments are in the linear regime, it is important to understand how the nature and the size of the defect affects the formation process of these solitonlike features. In a recent study [23] of the structural and optical properties of GaAs/AlAs microcavities grown by molecular beam epitaxy, it was shown that the most common pointlike defects were characterized by a circular or elliptical shape [24], due to Gallium droplets emitted occasionally during the growth

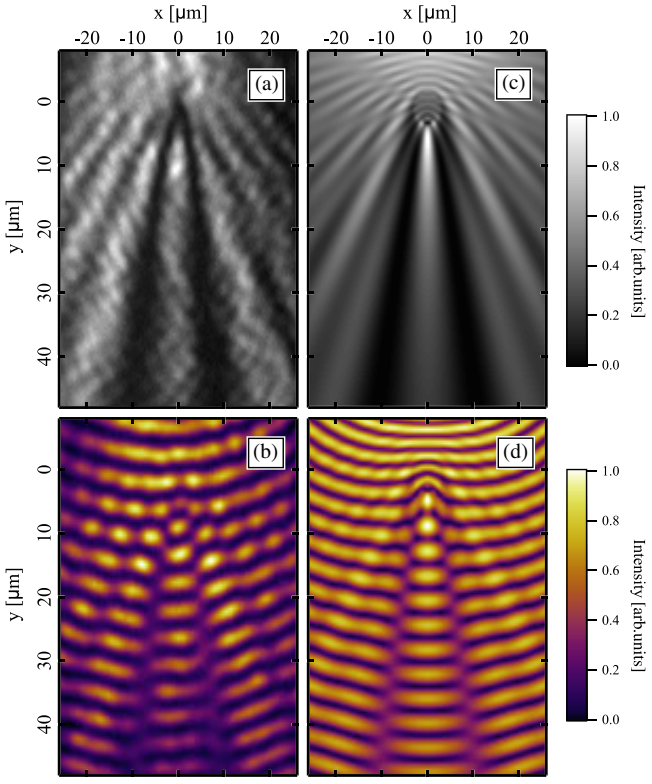

FIG. 1 (color online). Experimental (a),(b) and simulated (c),(d) real space intensity and interference patterns showing the two "soliton fingerprints" generated by the scattering of a beam with a pointlike defect: a dark notch in the intensity pattern together with π phase dislocations. In the images, the polaritons propagating downwards, along the y axis, are injected with a wave vector of 1.5 μm^{-1} and are scattered by a defect positioned 25 μm away from the excitation spots.

[25,26]. The presence of the defect has the effect of modifying the effective thickness of the cavity layer, which typically results in an attractive potential for the cavity mode inside the defect [24]. Consequently, the wave vector of the photonic mode in the region of the defect is higher than in the rest of the cavity.

The polariton scattering by the defect depends on the wave vector mismatch between the polaritons outside and inside the defect at the energy of excitation. When the energy shift of the defect photon mode with respect to the unperturbed cavity mode is large enough to make the coupling between them inefficient, the defect behaves like a hard scatterer and the spatial intensity distribution is similar to the complementary case of a single-slit diffraction [27]. In our case, however, there is a finite transmission through the defect, producing dark and bright traces with a more complicated phase pattern. As has been shown by Berry *et al.* [28,29], wave fronts resulting from interference can contain dislocation lines. In the case of a scattered beam, dislocations are composed of phase shifts at positions where the amplitude of the electromagnetic wave and, thus, the intensity vanishes, representing nodes of the wave. It is worth mentioning that nonlinearities are negligible close to nodes also in the nonlinear regime, and phase dislocations at zero intensity (i.e., at the dark notches) are features of both linear [30,31] and nonlinear waves. In our case, the analogy between linear and nonlinear waves goes beyond the mere observation of the same features and is effectively more profound. Indeed, as shown in [20] S4, the intensity, the phase jumps as well as the relative depth of the dark notches in the linear regime satisfy the same mathematical expression as in the quantum fluid case [15–18]. In particular, also in our linear system, the relative depth of the dark notches remains constant up to 42 μm (see [20], S4).

Beyond the qualitative discussion above, we performed simulations of the experiments, based on a numerical solution of the linear scattering problem using the classical theory of electromagnetism. The choice of such a model is justified by the fact that we operate in the linear regime and with a small exciton fraction of about 1%, such that the polariton dispersion is dominated by the cavity mode. In the model, we consider the propagation of quasi-two-dimensional photons with a parabolic dispersion in a cavity with a fixed width. The incident wave has been treated as coming from a linearly polarized pointlike source with polarization in the plane of the cavity. Defects have been modeled as disk-shaped perturbations of the cavity thickness resulting in an energy shift of the photon dispersion (see [20], S5). To model the defect parameters, which are not experimentally known, we use a disk shape with a radius of 3 μm and a polariton potential of -2.3 meV (consistent with Ref. [24]). Maxwell's equations are then solved using an expansion of the fields into the planar cavity eigenmodes in cylindrical coordinates fulfilling the boundary conditions for tangent components of electric and

magnetic fields on the interface between the cavity and the defect (see [20], S5). This linear wave dynamics model reproduces the intensity notch and the phase dislocation previously used as dark-soliton fingerprints. The results show a marked dependence on the geometry of the scattering problem, as shown in S6 [20]. In particular, the phase jump visible in the interference pattern depends on the direction of the incoming polariton wave relative to the defect (see [20] Fig. S7). On the other hand, the size of the defect relative to the polariton wavelength affects the formation of high-order phase dislocations (see [20] Fig. S8).

In a nonlinear cavity-polariton system, a polariton fluid has been predicted to flow almost unperturbed around the defect (i.e., disappearance of the features) or experience the nucleation of vortices and/or solitons at the position of the defect (i.e., appearance of the features), depending on the excitation density or on the energy of the pump [22]. We evaluated the possibility of observing these features, ascribed in the literature to dark solitons resulting from the interaction within the polariton fluid, in the absence of non-nonlinearities. Figures 2(a) and 2(b) show the phase and the intensity of solitonlike fingerprints in real space. Instead of increasing the excitation power, which has no effect in the linear regime, we tune the energy of the excitation beam and observe the appearance and disappearance of solitonlike features. As discussed above, the appearance of the intensity minima and phase dislocations is a result of interference

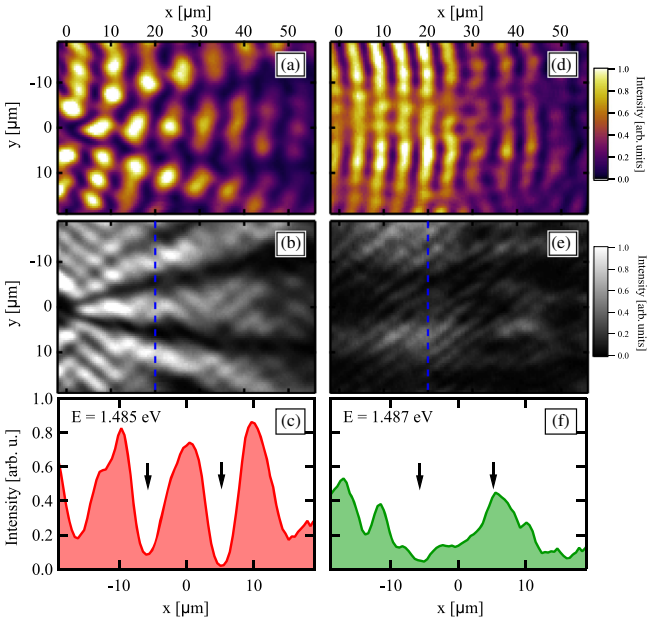

FIG. 2 (color online). Experimental interference (a),(c) and intensity (b),(d) showing the transition between the regime where the soliton features are well defined (1.485 eV) to a regime where they vanish (1.487 eV). The intensity profiles (e),(f) calculated along the blue dashed line, 20 μm away from the defect, confirm that the dark notches disappear when the energy of the excitation beam is increased. The two arrows indicate the positions of solitonlike fingerprints.

which is sensitive to the intensity and relative phase of contributing waves. The increase of the energy of the excitation beam by 2 meV causes an increase of the in-plane wave vector of the propagating polariton mode that, in turn, changes the interference condition so that the straight dark notches [Fig. 2(c)] and the phase dislocations [Fig. 2(d)] disappear. The wave vector dependence of such transitions will depend on the defect structure and the related bound polariton states [24], so that they could also be observed with decreasing wave vectors for other defects. Intensity profiles measured at a fixed distance from the defect [Figs. 2(e) and 2(f)] confirm the observed transition. Thus, it becomes apparent that the appearance or disappearance of solitonlike features, although independent of the excitation density, strongly depends on the wave vector of the propagating mode (see [20], S3). It is worth noting that an increase of the polariton density corresponds to an energy blueshift of the polariton dispersion. For polaritons excited resonantly with a given energy, this results in an increase of the polariton wave vector with decreasing density along the polariton propagation. Specifically, in nonresonantly excited experiments [32], this blueshift is dominated by the exciton density in the reservoir at high wave vectors. The interaction with the exciton reservoir is not a polariton-polariton interaction within the condensate which could provide the nonlinearity needed for the formation of solitons, but, instead, represents an external potential sculpting the polariton energy and gain landscape.

In a different experiment, we address the observation of half-soliton fingerprints, which requires polarization-resolved measurements. The intensity images [Figs. 3(a) and 3(b)] are measured using an excitation linearly polarized parallel to the y direction. The interferograms [Figs. 3(c) and 3(d)] are obtained by selecting the same polarization for the excitation and reference beam (see [20], S1 for details). The signature of an oblique dark half-soliton is a notch in only one circular polarization component [19,33]. We excite the sample with a linearly polarized beam and detect the two circular polarization components (σ_-, σ_+) separately. The measurements are performed with the same excitation energy (1.485 eV) and negative detuning (−29 meV) as in the previous case. The measured intensity and the interferogram for the σ_- component are given in Figs. 3(a) and 3(c), respectively. The images show the presence of a σ_- soliton fingerprint, indicated by the blue arrows, that is absent in the σ_+ component [Figs. 3(b) and 3(d)]. The same applies to the σ_+ counterpart, where a half-soliton fingerprint is observed only on the right side of the image.

By calculating the degree of circular polarization, given by $S_c = (I_{\sigma_+} - I_{\sigma_-})/(I_{\sigma_+} + I_{\sigma_-})$, with I_{σ_+} and I_{σ_-} being the measured intensities of the two components, we measure the pseudospin state inside the cavity [Fig. 4]. Here, if we look at the same position where the soliton features have been observed [Fig. 3] indicated by the black dotted lines in Fig. 4(a), we note the presence of a pair of oblique traces with

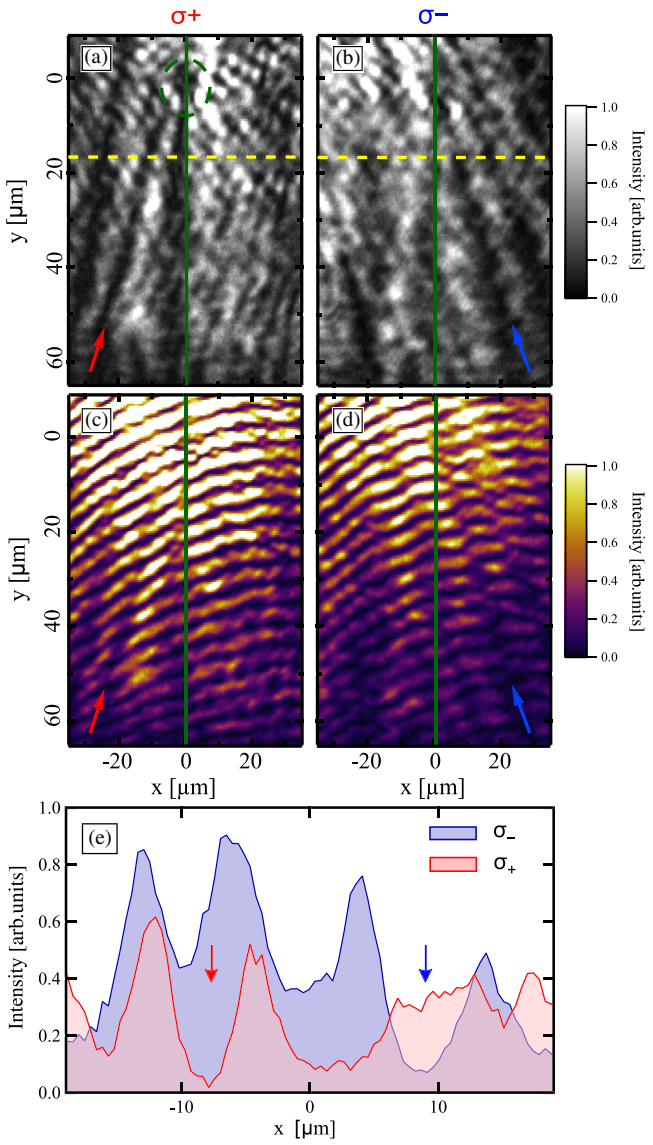

FIG. 3 (color online). Experimental intensity pattern (a)–(b) and real space interference (c)–(d) showing two half-soliton features as indicated by the arrows. The red and blue arrows indicate, respectively, the position of the σ_+ and σ_- soliton features: a dark notch with an associated phase jump present in only one circular component. The green vertical line is a guide for the eyes to distinguish the two different regions while the dashed circle in (a) indicates the defect. (e) The intensity profile extracts from the yellow dotted line displaying the two dark notches present, respectively, in only one opposite polarization basis, as indicated by the arrows.

opposite circular polarization, resembling the predictions and observations attributed to a polariton superfluid [19,33]. The high degree of circular polarization that we observe is due to the polarization splitting of transverse electric and transverse magnetic optical modes (TE-TM splitting) [34] (see [20], S7). The latter gives rise to the optical spin Hall effect [35] that has been observed in both polaritonic [36] and photonic microcavities [37]. In our

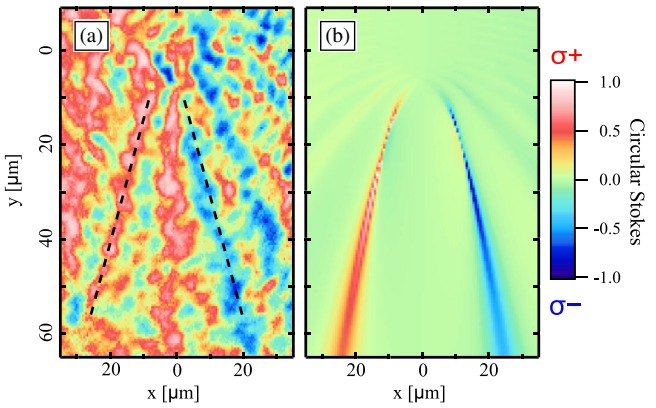

FIG. 4 (color online). Experimental (a) and simulated (b) circular Stokes parameter showing half-soliton features. The two black dotted lines correspond to the position of the dark notches present in Figs. 3(a) and 3(b).

simulations [Fig. 4(b)], a linearly polarized incoming beam propagates along the y direction and is scattered by a defect positioned at 25 μm away from the excitation spot, inducing the formation of two traces propagating in oblique directions. The detected field is a superposition of the incoming linearly polarized wave and the scattered wave. The TE-TM splitting of the optical mode in a photonic cavity is responsible for an anisotropy in the polarization flux, as previously shown on the same sample in Ref. [37]. Here, the same values of the TE-TM splitting have been used to perform the simulations. The polaritons scatter from the defect with wave vectors of equal modulus but in different directions both in the real and momentum space. Because of the birefringence induced by the TE-TM splitting, polaritons propagating in different directions experience different polarization rotation and shift. Polaritons traveling to the right gain a σ_+ component while polaritons traveling to the left gain a σ_- component. The anisotropy of the effect manifests itself in the intensity pattern, where it is possible to observe the features of an oblique soliton in one circular component and not in the other.

In conclusion, we have shown that the previously reported experimental signatures of oblique dark solitons and half-solitons in polariton condensates can be observed in the case of polaritons propagating in the linear regime. In our experiments these features are the result of the interference of the incoming wave with the waves scattered by the defect. Their phase jumps, and the relative depth of the dark notches satisfy the same analytical expression as in the polariton quantum fluid. In the case of the polarized counterpart (i.e., half-soliton-like features) the intrinsic TE-TM splitting of the cavity dispersion gives rise to oblique straight traces with opposite polarization.

Our results clarify that phase vortex lines in polariton propagation together with dark notches of constant relative depth in the intensity patterns, used as fingerprints of oblique-dark solitons and half-solitons in the literature, are present in the linear propagation regime. Consequently,

these features are necessary, but not sufficient, evidence to identify solitons. We believe a more reliable criterion for identifying dark solitons, based on the definition of solitons (i.e., solitary nonspreading wave), would be the size of the observed features which should be determined by the healing length of the condensate (see [20], S4 for details).

P. C. and P. L. acknowledge the Marie Curie ITNs Spinoptronics for funding. A. A. and P. L. acknowledge funding from Marie Curie ITN Clermont IV 235114. T. O. acknowledges financial support from the Grant Agency of Czech Republic, Project No. P204/10/P326. W. L. and P. L. acknowledge support by the EPSRC under Grant No. EP/F027958/1. P. C. acknowledges stimulating discussions with S. Portolan.

*pavlos.lagoudakis@soton.ac.uk

[1] G. I. Stegeman and M. Segev, Science **286**, 1518 (1999).
[2] M. Segev and G. Stegeman, Phys. Today **51**, No. 8, 42 (1998).
[3] Z. Chen, M. Segev, and D. N. Christodoulides, New J. Phys. **75**, 086401 (2012).
[4] A. Barthelemy, S. Maneuf, and C. Froehly, Opt. Commun. **55**, 201 (1985).
[5] M. Segev, B. Crosignani, A. Yariv, and B. Fischer, Phys. Rev. Lett. **68**, 923 (1992).
[6] K. Hayata and M. Koshiba, Phys. Rev. Lett. **71**, 3275 (1993).
[7] M. Nakazawa and K. Suzuki, Electron. Lett. **31**, 1076 (1995).
[8] P. D. Miller, Phys. Rev. E **53**, 4137 (1996).
[9] T. Tsuzuki, J. Low Temp. Phys. **4**, 441 (1971).
[10] Y. Kivshar, IEEE J. Quantum Electron. **29**, 250 (1993).
[11] J. Denschlag, J. E. Simsarian, D. L. Feder, C. W. Clark, L. A. Collins, J. Cubizolles, L. Deng, E. W. Hagley, K. Helmerson, W. P. Reinhardt, S. L. Rolston, B. I. Schneider, and W. D. Phillips, Science **287**, 97 (2000).
[12] J. Kasprzak, M. Richard, S. Kundermann, A. Baas, P. Jeambrun, J. M. J. Keeling, F. M. Marchetti, M. H. Szymanska, R. André, J. L. Staehli, V. Savona, P. B. Littlewood, B. Deveaud, and L. S. Dang, Nature (London) **443**, 409 (2006).
[13] A. Amo, J. Lefrère, S. Pigeon, C. Adrados, C. Ciuti, I. Carusotto, R. Houdré, E. Giacobino, and A. Bramati, Nat. Phys. **5**, 805 (2009).
[14] A. Amo, D. Sanvitto, F. P. Laussy, D. Ballarini, E. d. Valle, M. D. Martin, A. Lemaître, J. Bloch, D. N. Krizhanovskii, M. S. Skolnick, C. Tejedor, and L. Viña, Nature (London) **457**, 291 (2009).
[15] A. Amo, S. Pigeon, D. Sanvitto, V. G. Sala, R. Hivet, I. Carusotto, F. Pisanello, G. Leménager, R. Houdré, E. Giacobino, C. Ciuti, and A. Bramati, Science **332**, 1167 (2011).
[16] G. Grosso, G. Nardin, F. Morier-Genoud, Y. Léger, and B. Deveaud-Plédran, Phys. Rev. Lett. **107**, 245301 (2011).
[17] G. Grosso, G. Nardin, F. Morier-Genoud, Y. Léger, and B. Deveaud-Plédran, Phys. Rev. B **86**, 020509 (2012).
[18] B. Deveaud, G. Nardin, G. Grosso, and Y. Léger, in *Physics of Quantum Fluids*, Springer Series in Solid-State Sciences Vol. 177, edited by A. Bramati and M. Modugno (Springer Berlin, 2013), pp. 99–126.
[19] R. Hivet, H. Flayac, D. D. Solnyshkov, D. Tanese, T. Boulier, D. Andreoli, E. Giacobino, J. Bloch, A. Bramati, G. Malpuech, and A. Amo, Nat. Phys. **8**, 724 (2012).
[20] See Supplemental Material at http://link.aps.org/supplemental/10.1103/PhysRevLett.113.103901 which includes Refs. [38-42], for detailed description of the experimental setup (S1), the power dependence measurements and calculation of the polariton density and renormalization (S2), the energy dependent measurements for a different defect (S3), the evaluation of the dark solitons conditions for measurements in the linear regime (S4), the theory for the cavity mode scattering by a point defect (S5), the dependence of the solitonlike features on the scattering geometry (S6), the half-solitonlike features caused by TE-TM splitting (S7).
[21] H. Deng, G. Weihs, D. Snoke, J. Bloch, and Y. Yamamoto, Proc. Natl. Acad. Sci. U.S.A. **100**, 15318 (2003).
[22] S. Pigeon, I. Carusotto, and C. Ciuti, Phys. Rev. B **83**, 144513 (2011).
[23] J. Zajac, W. Langbein, M. Hugues, and M. Hopkinson, Phys. Rev. B **85**, 165309 (2012).
[24] J. Zajac and W. Langbein, Phys. Rev. B **86**, 195401 (2012).
[25] K. Fujiwara, K. Kanamoto, Y. Ohta, Y. Tokuda, and T. Nakayama, J. Cryst. Growth **80**, 104 (1987).
[26] N. Chand and S. Chu, J. Cryst. Growth **104**, 485 (1990).
[27] E. Hecht and A. Zajac, *Optics* (Addison-Wesley, Reading, MA, 1982).
[28] M. V. Berry, in *Huygens' Principle 1690-1990: Theory and Applications: Proceedings of an International Symposium, the Hague/Scheveningen, 1990*, edited by H. P. Blok, H. A. Ferwerda, H. K. Kuiken (Elsevier Science Publishers, Amsterdam, 1992), pp. 97–111.
[29] M. V. Berry, J. F. Nye, and F. J. Wright, Phil. Trans. R. Soc. A **291**, 453 (1979).
[30] S. V. P. Senthilkumaran, Opt. Commun. **283**, 2767 (2010).
[31] G. Ruben and D. M. Paganin, Phys. Rev. E **75**, 066613 (2007).
[32] G. Tosi, G. Christmann, N. G. Berloff, P. Tsotsis, T. Gao, Z. Hatzopoulos, P. G. Savvidis, and J. J. Baumberg, Nat. Phys. **8**, 190 (2012).
[33] H. Flayac, D. Solnyshkov, and G. Malpuech, Phys. Rev. B **83**, 193305 (2011).
[34] G. Panzarini, L. C. Andreani, A. Armitage, D. Baxter, M. S. Skolnick, V. N. Astratov, J. S. Roberts, A. V. Kavokin, M. R. Vladimirova, and M. A. Kaliteevski, Phys. Rev. B **59**, 5082 (1999).
[35] A. Kavokin, G. Malpuech, and M. Glazov, Phys. Rev. Lett. **95**, 136601 (2005).
[36] C. Leyder, M. Romanelli, J. P. Karr, E. Giacobino, T. C. H. Liew, M. M. Glazov, A. V. Kavokin, G. Malpuech, and A. Bramati, Nat. Phys. **3**, 628 (2007).
[37] M. Maragkou, C. E. Richards, T. Ostatnický, A. J. D. Grundy, J. Zajac, M. Hugues, W. Langbein, and P. G. Lagoudakis, Opt. Lett. **36**, 1095 (2011).
[38] L. G. A. El, A. Gammal, and A. M. Kamchatnov, Phys. Rev. Lett. **97**, 180405 (2006).
[39] M. Segev, Opt. Photonics News **13**, 27 (2002).
[40] A. D. Jackson, G. M. Kavoulakis, and C. J. Pethick, Phys. Rev. A **58**, 2417 (1998).
[41] W. Langbein, Phys. Rev. B **70**, 205301 (2004).
[42] A. W. Snyder and J. D. Love, *Optical Waveguide Theory* (Chapman and Hall, London, 1983).